Palacky University in Olomouc
Faculty of Science
Department of Experimental physics

Self-Report

Study of spectra of top quarks produced in pairs in experiment ATLAS

Author	**Josef Pácalt**
Study programme:	Physics
Specialization:	Applied Physics
Study form:	Daily
Supervisor:	Mgr. Jiří Kvita, PhD
Date of submission:	January 2023

The ATLAS Detector

The ATLAS detector situated at the LHC at CERN is a multipurpose cylindrical detector for measurement of properties of particles, studies of high energy physics as well as signs of new physics. There are two beam pipes at the LHC in which two beams of protons are circulating in opposite directions. These beams are crossing in four interaction points where the detectors are build. Protons circulating in LHC are colliding in bunches for enhancing the chance of collision, each bunch containing approximately 10^{11} protons and colliding with frequency up to 40 MHz. There are multiple collisions of protons happening within each bunch crossing, a process called pile-up (PU), but usually only few of them can be classified as a "hard" process. The "hard" process is the creation of high-transverse momentum objects in proton-proton collision. These can be heavy quarks, leptons or bosons which are objects of interest for scientists and there is need of precise measurement of their properties or precise measurement of properties of their decay products.

The ATLAS uses right-hand coordinate system with x-axis pointing to the center of the ring, y-axis pointing up and z-axis pointing alongside the ring. This system of coordinates is also used for the description of events inside experiments. The experiments often use A-side and C-side notation, which is shorthand of clockwise and anticlockwise direction from the center of the experiment detector respectively.

Standard Model and the Top Quark

The Standard Model (SM) is a theory of particle physics where the particles consists of three generation of quarks and leptons and interactions mediated by the corresponding gauge bosons. The last discovered particle is the Higgs boson, which in theory gives the other particles its mass by interaction with the Higgs field [1, 2, 3]. The overview of known elementary particles is shown in Fig. 1.

Top Quark

The top quark is the heaviest quark in the SM and its discovery was announced in 1995 by the CDF and D0 experiments at the Tevatron collider [5, 6]. The experiments at Tevatron were the first to measure the top quark properties. Later, when the LHC started to operate, ATLAS and CMS experiments joined the efforts [7]. The top quark mass combined results from aforementioned experiments is $M_{\mathrm{t}} = 172.69 \pm 0.30$ GeV [8], which is an important parameter in studies of the stability of the universe [9], thus the interest in increasing the precision of the measurement. The top quark, with its large mass in comparison to other quarks and very short lifetime, decays before the hadronization can occur, thus the measurement of its properties can not be done directly. The large mass is responsible for largest coupling to the Higgs boson in comparison to the rest of the quarks, thus being important for measuring Higgs boson properties and for BSM theories.

Channels and Topologies

The production of the top anti-top quark pairs is separated into decay channels by the final products of the decay. The majority of top quarks and anti-top quarks, around

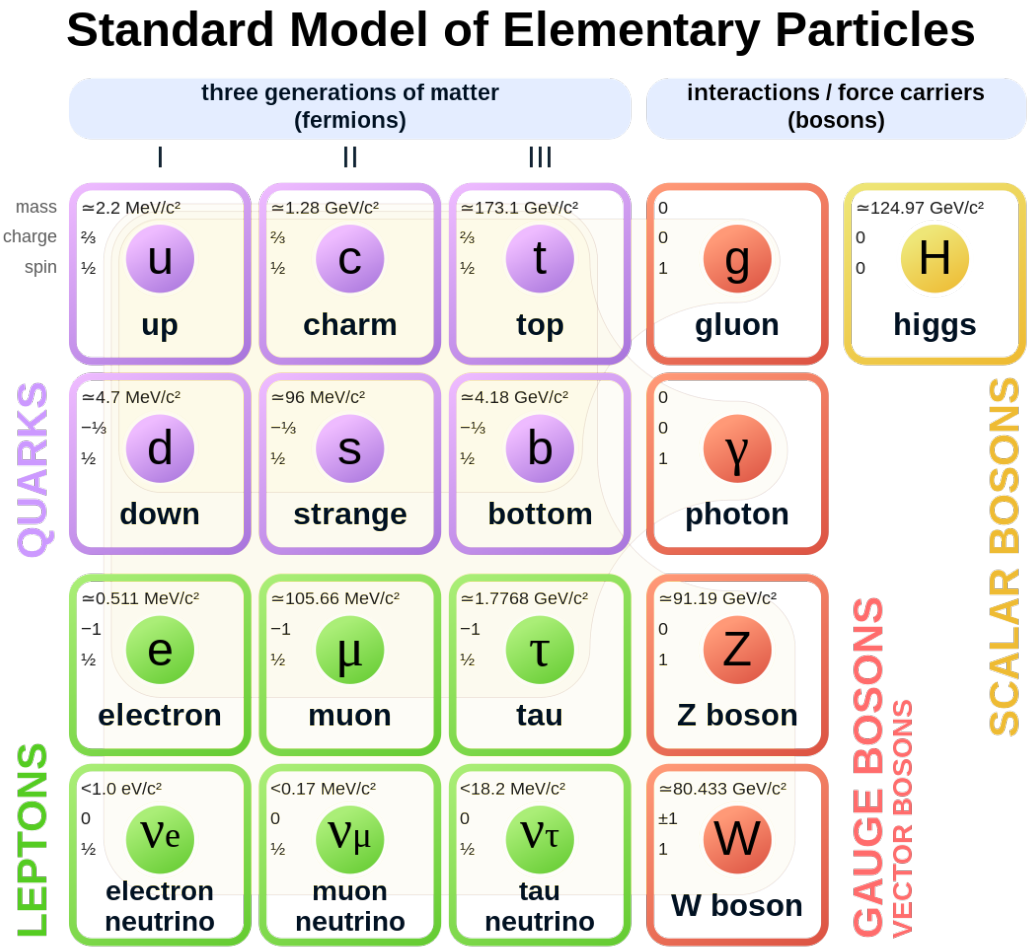

Figure 1: Overview of the Standard Model basic particles with additional information about their charge, mass and spin. The figure was taken from [4].

99%, decay to the W boson and bottom or anti-bottom quark and the decay happens before the top quark hadronizes or reaches the detection surface. Furthermore, the W boson decay either to the lepton and corresponding neutrino (leptonicaly decaying W boson) or quark anti-quark pair (hadronicaly decaying W boson). Similar notation is used to top quarks, in other words, leptonically decaying top quark has its daughter W boson decayed leptonically. The final decay products of W bosons determine the channel. There are two W bosons in each $t\bar{t}$ event which both decay either hadronically or leptonically leading to three combinations. If both W decayed hadronically, then we classify the event as an event in all-hadronic channel, if both W bosons decay leptonically, then the event belongs to the di-lepton channel. The semi-leptonic channel is defined by combination of one hadronically decaying W boson while the other W boson decay leptonically, which is the explored channel in this work.

The topology classification is needed for the analysis purposes after the process and channel is established. The topology is defined by the position of final states products in the detector, which is highly correlated to the momentum of the decayed particle. In the resolved topology all decay products are separated in the detector, no overlap of the jets is allowed. This topology often corresponds to decayed particles with lower momentum. The opposite boosted topology, where all product of the decay are reconstructed as one object, large jet, is corresponding to the decay of particles with large momentum. The semi-boosted topology lies in between those two, where some products are reconstructed as one object as in the boosted topology into the large jet, but rest of decay products are reconstructed separate as in the resolved topology.

Two hypothetical particles, vector boson Z' and scalar boson y_0, are used for better exploration of this energy region. These particles are used as probing mechanism of reconstruction and it is possible to tune energy of the event by setting its mass. The studied process can be described as follows: $pp \to Z'(y_0) \to t\bar{t}$, $t_1 \to W + b \to \nu + \ell + b$, $t_2 \to W + b \to b + q + \bar{q}$. Topologies mentioned above are different in final products observed in detector especially on the hadronicaly decaying side. The resulting jets, typical for resolved topology coming from hadronic decay, are not overlapping each other in the detector thus forming small jets, see Fig. 2 a) for the graphical description. This behavior is standard for events from the beginning of energetic spectrum of $M_{Z'}$. In contrary, the boosted topology exploits the overlap of products and part of the definition of this topology is large jet, which contains all final products of hadronicaly decaying top quark, see Fig. 2 d) for schematic visualization. It is obvious, that there is condition on sufficient energy of top quark for this topology to have the final products collimated enough to form large jet. In between of those topologies lies interval of energy spectrum, where the resolved events are diminishing, but the energy is not yet high enough to form boosted event. This transition region between those two topologies is preferred by the semi-boosted and semi-boosted mixed topology, where two products of hadronicaly decaying top quark form large jet, but one product lies outside this large jet and forms single small jet, the difference between those two topologies is in the origin of the escaping product. The decaying schemes and final products of studied events for semi-boosted and semi-boosted mixed topology are shown on figure 2, b) and c) respectively.

Leptons and Missing Transverse Energy

Leptons and neutrinos are crucial for reconstructing the W bosons, which may decay into a lepton and a neutrino pair. The detectors are able to directly detect

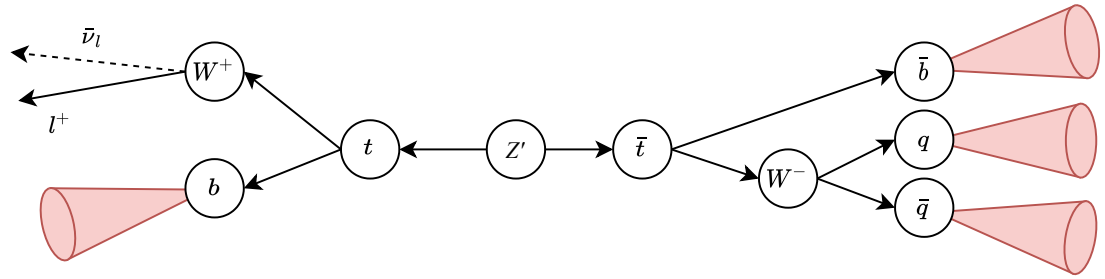

a)

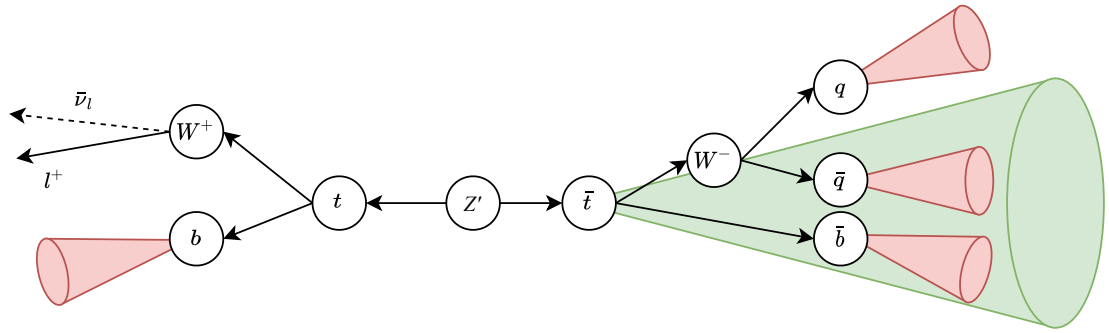

b)

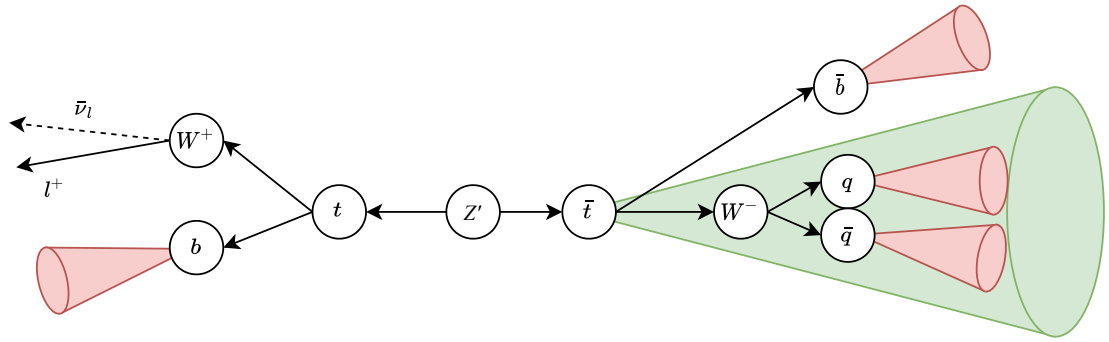

c)

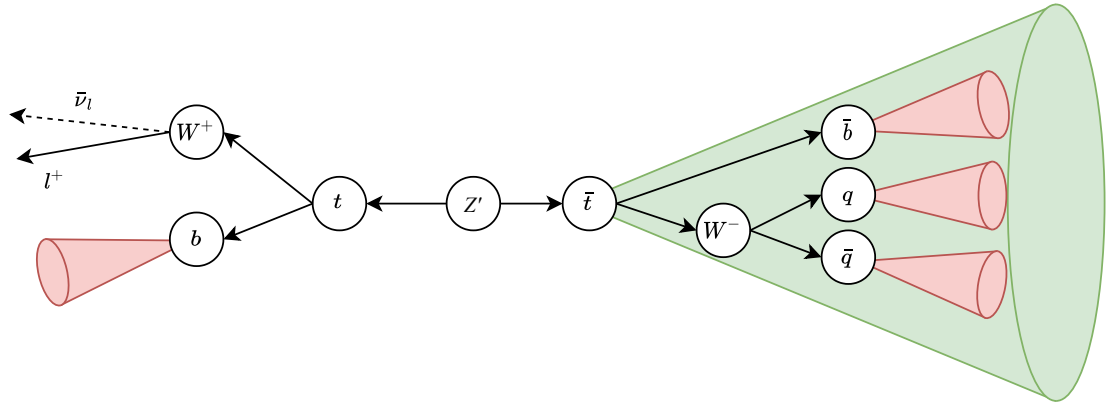

d)

Figure 2: Schematics of an event $Z' \to t\bar{t}$ decay in resolved a), semi-boosted mixed b), semi-boosted c) and boosted d) topology.

leptons with exception of τ lepton, which decay before entering the detection areas of the detector although products of the decay are detected and there are method for its reconstruction. The detection of neutrinos is next to impossible and ATLAS detector is unable to detect them. However, there is a concept in the reconstruction phase which replaces direct measurement of the neutrinos (at least their transverse momentum) by measurement of the imbalance in transverse momentum by summing four-vectors of all detected particles, which should equal to zero by definition due to the vanishing transverse momentum contribution of the incoming protons. This imbalance of momentum is caused by neutrinos escaping the detection and is equal to the negative sum of neutrino four-vectors from the studied final-state, called the missing transverse energy (MET), or momentum as the mass of neutrinos is negligible, and defined as follows

$$\overrightarrow{E}_{\mathrm{T}}^{\mathrm{miss}} = (-\sum_{\mathrm{i}} p_{\mathrm{x,i}}, -\sum_{\mathrm{i}} p_{\mathrm{y,i}}), \tag{1}$$

where $\overrightarrow{E}_{\mathrm{T}}^{\mathrm{miss}}$ is the missing transverse momentum vector, $\sum_{\mathrm{i}} p_{\mathrm{x,i}}$ is summed contribution of all detected particles momentum alongside x-axis and $\sum_{\mathrm{i}} p_{\mathrm{y,i}}$ is summed contribution of all detected particles momentum alongside y-axis. Both leptons and MET, are used in the reconstruction of the top anti-top quark pair events in the ATLAS analyses and in this work.

Jets

Most of the physics results performed at the ATLAS detector use jets as physics objects. The reconstructed objects hadronic final states known as jets, are products of dedicated jet reconstruction algorithms. There are three jet levels, as illustrated in Fig. 3. Parton level jet is constructed from constituents before the hadronization, *i. e.* quarks and gluons, next level is a particle level jet, which is built using stable particles, third level is the detector level, where the input for the jet algorithm are deposits of the energy in calorimeter.

Jet Reconstruction

The reconstructed jet at any level can be described by its momentum and angular variables used to evaluate the direction of jet. The first variable of interest is the transverse momentum (p_{T}), which is the momentum of the particle in the transverse plane with respect to the direction of the incoming colliding protons. The sum of transverse momenta of all particles in event is expected to be zero, which results from the law of conservation of momentum. The higher the transverse momentum is, the higher energy deposit in calorimeter is for a fixed direction of the jet. Two angular variables are used for the description of the direction of the jet. First variable is the azimuthal angle ϕ in the transverse plane in regard to the direction of incoming protons in the detector. The cylindrical ATLAS detector is symmetric in this variable which thus has no influence on the reconstruction of the jet. Second variable called pseudorapidity describes the elevation of the jet from the direction of the incoming protons and is defined by the following formula:

$$\eta = -\ln\tan\frac{\theta}{2}, \tag{2}$$

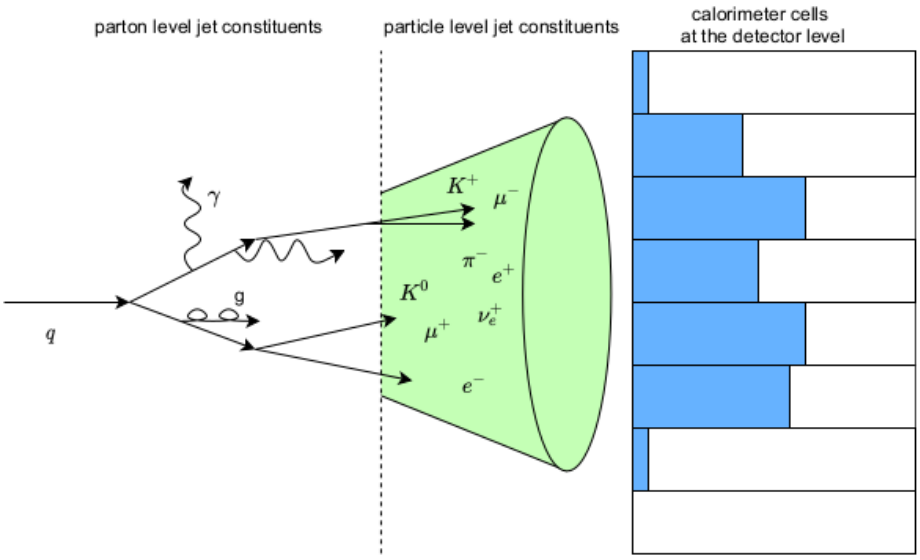

Figure 3: The visualization of the particle reconstruction levels from parton (particles before hadronization) through particle level (particles after the hadronization) to the detector level (measured particle tracks and deposits in calorimeters).

where θ is the angle or between the jet momentum direction and the beam axis, but the angle measured in laboratory frame may differ by the boost of the particle alongside the beam axis and is denoted as production angle θ^*. The jet direction lies in the transverse plane to the direction of the incoming colliding protons for $\eta = 0$. There are several jet reconstruction algorithms. These algorithms use iterative method for clustering jet constituents [10]. The condition for clustering is a metric defined as follows:

$$d_{\mathrm{i,j}} = \min(p^{\mathrm{q}}_{\mathrm{T,i}}, p^{\mathrm{q}}_{\mathrm{T,j}}) \frac{\Delta y^2_{\mathrm{i,j}} + \Delta \phi^2_{\mathrm{i,j}}}{R^2}, \tag{3}$$

where $p_{\mathrm{T,i}}$ and $p_{\mathrm{T,j}}$ are transverse momenta of examined constituents i and j, q is the parameter for different clustering algorithms and R is the distance parameter, roughly corresponding to the radius the resulting jet area in the calorimeter and y is pseudorapidity defined in high energy physics as

$$y = \frac{1}{2} \ln \frac{E + p_{\mathrm{z}}}{E - p_{\mathrm{z}}}, \tag{4}$$

where E is energy and p_{z} is longitudinal momentum of the studied object, corresponding to direction alongside the LHC ring and denoted as the z-component of the momentum. Pseudorapidity converges to the rapidity in approximation $m \ll p$, where m is mass and p is momentum of the studied object. The algorithm then sums the four-momenta of the two constituents with smallest $d_{\mathrm{i,j}}$ and removes them from the list of objects for reconstruction and adds the resulting constituent into the list and repeats the procedure.

Private Analysis

A private analysis is described in this chapter. It aims to study the process where top anti-top quark pair decays in the ℓ + jets channel and its performance in different topologies with focus on the semi-boosted one. The motivation for this study is the enhancement of the measurable events by adding the semi-boosted and semi-boosted mixed topology into the analyses in the top anti-top quark final states, which would be otherwise discarded. The comparison of the performance of the unfolding procedure between topologies is present with its evaluation of influence on the signal strength of the presence of the simulated hypothetical particle. The hypothetical particles Z' and y_0 are used as a probe, where the different values of mass of the hypothetical particle are used to tune in the desired energy region for topology studies. Its reconstructed mass peak is used as the tool for resolution studies. This chapter contains description of preparation of the simulated samples, the simulation of the ATLAS detector, private JES correction derivation and the event selection followed by the reconstruction description in all four studied topologies.

The analysis framework consists of three main parts: The preparation of the samples, the selection and reconstruction of the selected events and the unfolding procedure. The samples are prepared with the MadGraph5 package and the simulation of the ATLAS-like detector is performed with the DELPHES package. The framework has been implemented with a private algorithm for JES factors derivation and application. Jets are enter the events selection after the application of this JES correction and tagging on the original particle is performed on the large jets enhance the performance of the event selection.

Generated Samples

Samples were simulated by the MadGraph5 2.6.4 software package [11] with specialized model package (`Abelian_Higgs_Model_UFO`) for simulation of a hypothetical vector particle Z' and scalar particle y_0 [12, 13, 14]. Samples were prepared for different values of mass of this hypothetical particle, ranging in interval of 500 – 1000 GeV.

All samples hold information from the both detector and particle levels. The detector level corresponds to measured data with imperfections as coming from a close-to-real detector. Particle level describes particles just before entering the detector.

Events are simulated to correspond to proton-proton future collisions at the Large Hadron Collider (LHC) at CERN with the center of mass energy $\sqrt{s} = 14$ TeV. Jets are the experimental signatures of hadronic final states of quarks and gluons, which form particle showers entering the detector and leaving their energy there. Jet constituents are clustered energy deposits in calorimeters or stable particles at the particle level. Small jets, with distance parameter $R = 0.4$, in all signal and background samples were generated with a cut on the transverse momentum on generator level of $p_{\mathrm{T,SJ}} > 20$ GeV to increase amount of events of interest in the detector simulation. Samples containing the hypothetical particle Z', Wbb+jets background sample and a $t\bar{t}$ sample were all generated at the next-to-leading order (NLO) of QCD, while samples with the hypothetical particle y_0 and $WWbb$+jets background sample were generated at the leading order (LO) only. The y_0 was simulated at the leading order due to the triangle loop process for which the NLO level was unavailable in the MadGraph5 simulation and the cause for the $WWbb$+jets background sample is a small contribution to the events reconstructed by the analysis framework.

The luminosity of the sample is calculated as follows:

$$L = \frac{N}{\sigma}, \tag{5}$$

where L is the luminosity of the sample, N is the number of generated events and σ is cross-section of the sample.

Spectra from different samples may be weighted to the same luminosity for comparison purposes or for the admixture for the unfolding procedure. The weight is defined as $L_{\text{ref}} = wL_{\text{w}}$ where L_{ref} is the luminosity of the reference sample, w is the weight for spectra scaling and L_{w} is the luminosity of the weighted spectrum sample.

Private Jet Energy Scale

The DELPHES-provided JES correction for large jets is not used at all, but the DELPHES JES (JetJES collection) for small jets is, but the ratio of the small jet energy on the detector level over the energy of the matched particle jet plotted against the small jet η on the detector level is showing large dependence on η, thus, the small jets are corrected for this phenomenon in same manner as large jets by private additional JES correction factors.

The jet energy scale correction used in the analysis framework has been derived from the $t\bar{t}$ sample specially generated for this purpose with lower cut on the minimal transverse momentum of jets (15 GeV) to enhance performance of JES correction for jets with lower transverse energy, namely around 25 GeV. The JES factor derivation is performed in a similar manner to the ATLAS working group method and amplified both large and small DELPHES jets.

Event Selection

Events considered in the analysis are reconstructed at two levels; once with the DELPHES ATLAS detector simulation, forming detector level spectra, and at the particle level. The event selection and the requirements differ slightly for the reconstruction level and for the boosted, semi-boosted, semi-boosted mixed and resolved topologies and are described below.

Missing Transverse Energy and Lepton Selection

The missing transverse energy ($E_{\text{T,miss}}$) used in the private analysis is defined in same manner as in equation 1. The magnitude of the missing transverse energy is required to be $E_{\text{T,miss}} > 25$ GeV for all topologies as well as for both the detector and the particle levels. This ensures that only events in which neutrinos carry away a considerable amount of energy from the decay are chosen for the analysis. This is a standard requirement for the missing energy in most of top quark analyses in channels including leptons.

The second condition in the selection order is the requirement on the lepton (muon or electron) transverse momentum, namely $p_\ell > 25$ GeV. Similar value is also commonly used in top quark analyses. Tau leptons are not directly considered in the simulation as they decay before they enter the detector, but their leptonic decay products (ℓ, μ) are. In case there are more electrons or muons fulfilling this requirement,

only the electron or muon with the highest transverse momentum is taken into account. These requirements are the same for all topologies. Events are separated to an electron or a muon channel by the flavor of the selected lepton. The lepton may radiate low energy photons which are highly collimated. The separation of those radiated photons and the lepton is below the resolution of the detector and the photon energy is added by construction at the detector level. The lepton dressing procedure is performed at the particle level reconstruction to correct for this phenomenon. Photon four-vectors, fulfilling the condition of the angular separation threshold $\Delta R_{\gamma,\ell} = \sqrt{\Delta\eta^2_{\gamma,\ell} + \Delta\phi^2_{\gamma,\ell}} < 0.1$, are added to the lepton four-vector.

Large Jet Selection

The large jet four-vector is the result of the reconstruction with the anti-k_t algorithm with a distance parameter $R = 1$. A private jet energy scale correction is applied to the detector level large jet before the selection, derived on the $t\bar{t}$ sample. The magnitude of the jet energy scale correction is about 5% depending on η and p_{T}. The transverse momentum of large jets is required to be $p_{\mathrm{T,LJ}} > 100$ GeV. This condition helps to reduce the number of events with jets not coming from top quark decays. Furthermore, all large jets are considered in the pseudorapidity range $|\eta| < 2.5$. This constraint ensures in practice better jet identification as the forward region of the detector is not instrumented for tracking and has a worse energy resolution. The isolation criterion of jets from the lepton ensures that the selected lepton is not contained within the large jet by following the requirement of $\Delta R_{\mathrm{LJ},\ell} = \sqrt{\Delta\eta^2_{\mathrm{LJ},\ell} + \Delta\phi^2_{\mathrm{LJ},\ell}} > 1$. All these requirements are applied to all three topologies[1] and both the detector and the particle levels. Each large jet is then probed for the top quark and W boson tagging, first for the hypothesis as coming from the top quark decay, then, in the semi-boosted topology, as coming from the W boson decay and in case none of the tagging was successful, the event is then considered as a candidate for the semi-boosted mixed or the resolved topology.

Tagging for the boosted topology is based on the constraint on the mass of the large jet 110 GeV$< M_{\mathrm{LJ}} <$ 240 GeV and a constraint combining the large jet mass and a jet substructure variable $\tau_{3,2}$ [15], describing the possibility of finding three small jets inside the studied large jets rather than two small jets, as $M_{\mathrm{LJ}}/\tau_{3,2} > 256$ GeV. The value for the second constraint was added to avoid background jets, *e.g.* a large jet from the W boson.

Small Jet Selection

The general requirements for the small jet selection are on the transverse momentum $p_T > 25$ GeV and the isolation from the selected lepton $\Delta R_{\mathrm{SJ},\ell} > 0.5$. The private jet energy scale correction is applied to detector level small jets before the selection, which was derived on the $t\bar{t}$ sample on top of the DELPHES default jet energy scale. The magnitude of this residual jet energy scale correction is about 2%. The b-tagging of the small jets is done by the DELPHES simulation at the detector level and by the requirement of containing a B-hadron at the particle level by fulfilling the requirement of $\Delta R_{\mathrm{SJ,B-had}} < 0.4$.

[1] There is no large jet in the resolved topology.

The small jet for the reconstruction of the leptonically decaying top quark has to fulfill the angular condition $\Delta R_{\mathrm{SJ},\ell} < 2$, which ensures that it lies in the vicinity of the selected lepton, and must be b-tagged. The large jet isolation condition $\Delta R_{\mathrm{SJ,LJ}} > 1.5$ applies to all topologies with the exception of the resolved topology, where there is no large jet. Such a selected small jet is then removed from the jet collection and from further consideration. This is the only selected small jet in case of the boosted topology.

For the reconstruction of the hadronically decaying top quark in the semi-boosted topology a small b-tagged jet is required in the vicinity to the selected large jet $1 < \Delta R_{\mathrm{SJ,LJ}} < 1.5$. Thus a partial overlap between the selected large jet and the considered small jet is allowed, *i.e.* the selected b-tagged small jet can be partially contained in the selected large jet.

The conditions for the semi-boosted mixed topology are similar to the conditions for the semi-boosted topology. The vicinity condition to the large jet remains unchanged but the small jet is required not to be b-tagged. This condition together with the b-tag of the selected large jet ensures the correct selection for this topology.

The resolved topology selection is tried as the last option before the event is discarded. The reconstruction of the hadronically decaying top quark in the resolved topology requires three small jets, one of them b-tagged. The algorithm first takes two small non-b-tagged jets with the highest transverse momentum and tests their invariant mass $M_{\mathrm{SJ,SJ}} < 120$ GeV to avoid dijets not corresponding to the mass of the W boson. Then it adds the four-vector of the remaining b-tagged jet[2]. If such three jets are found, the event is accepted.

Top Quark Pair Reconstruction

The top quark pair reconstruction is independent on the event on the complementary reconstruction level, thus the different reconstructed topology event on the detector and the particle level is not forbidden. Another parallelization in reconstruction is in the lepton selection, where the event with muon and electron is reconstructed independently if both of them fulfill the selection criteria. Parallelization in the lepton selection and independence on the complementary event is used to increase the number of reconstructed events and efficiency of the algorithm. The topology matching between the detector and particle level is only performed for the spectra undergoing the unfolding procedure.

Reconstruction of Leptonically Decaying Top Quark

Reconstruction of leptonically decaying part of event is same for all topologies. First, the condition on missing energy is tested, then the presence of the selected electron or muon is verified. The object reconstructed from four-momenta of the chosen lepton and missing energy, considered as the energy of undetected neutrino, is corresponding with W boson, but due to uncertainty coming from not knowing the longitudinal component of neutrino momentum there are up to two possible values of the W boson longitudinal momentum component. The ambiguity is caused by the calculation from condition $M_{\ell,\nu} = M_{\mathrm{W}}$, where$M_{\ell,\nu}$ is combined invariant mass of the reconstructed W boson from lepton and missing energy, which leads to the quadratic

[2]One b-tagged jet is used in the reconstruction of the leptonically decaying top quark.

equation. The more central value of the longitudinal component of reconstructed neutrino momentum is usually selected in ATLAS collaboration analyses. The last object needed for the leptonically decaying top quark reconstruction is the selected b-tagged small jet. The leptonically decaying top quark four-momentum is then obtained as the combination of four-momenta of the reconstructed W boson object and the selected small jet. In case that the algorithm was able to reconstruct the leptonically decaying top quark with selected electron and muon simultaneously, the top quark candidate reconstructed from lepton with higher transverse momentum is selected. Reconstruction of the leptonically decaying top quark is identical for the detector and particle level, with exception of the small jet b-tagging.

Reconstruction of Hadronically Decaying Top Quark.

The reconstruction of the hadronically decaying top quark is different for each of the topologies. The algorithm first tries to find the boosted topology top quark pair candidate, in case of failure it attempts to find the semi-boosted topology pair and in case of subsequent failure it tries the semi-boosted mixed topology selection. The resolved topology top quark pair reconstruction takes place only if all previous topology conditions fail. The studied event is discarded only in case in which algorithm was unsuccessful in reconstruction of event in all topologies.

The reconstruction of the hadronically decaying top quark in the boosted topology is based on selection of top tagged large jet, as mentioned in previous section, which is considered as the top quark candidate, because it should contain most of the decay products corresponding to the original particle.

The reconstruction of the hadronically decaying top quark in the semi-boosted topology is similar but the selected tagged large jet corresponds to the W boson instead to the top quark as in the previous case. Thus, the small jet tagged by the reconstruction algorithm as containing products of B-hadron decay is needed to complete the four-momentum of the reconstructed top quark.

The reconstruction of the hadronically decaying top quark in the semi-boosted mixed topology is performed by summing one large b-tagged jet and one non-b-tagged small jet four-vectors. The invariant mass of such a large jet does not produce a peak corresponding to any particle but in the combination with the selected small jet the resulting invariant mass peak should correspond to the one of the top quark.

The reconstructed hadronically decaying top quark four-momentum in the resolved topology is the sum of four-momenta of three selected small jets as described in previous section. As there is no selected large jet but only small jets, this topology is the most prone one to the miscombination of jets, which is one of the reasons of slightly worse resolution in the reconstruction of the top quark pair invariant mass.

Finally, the reconstructed top anti-top quark pair four-momentum is obtained as a combination of four-momenta of the reconstructed hadronically and leptonically decaying top quark.

Results

Results from selection and reconstruction are presented in this section. The signal sample with the hypothetical particle y_0 with decay width of 10% of its invariant mass is chosen for the results presentation.

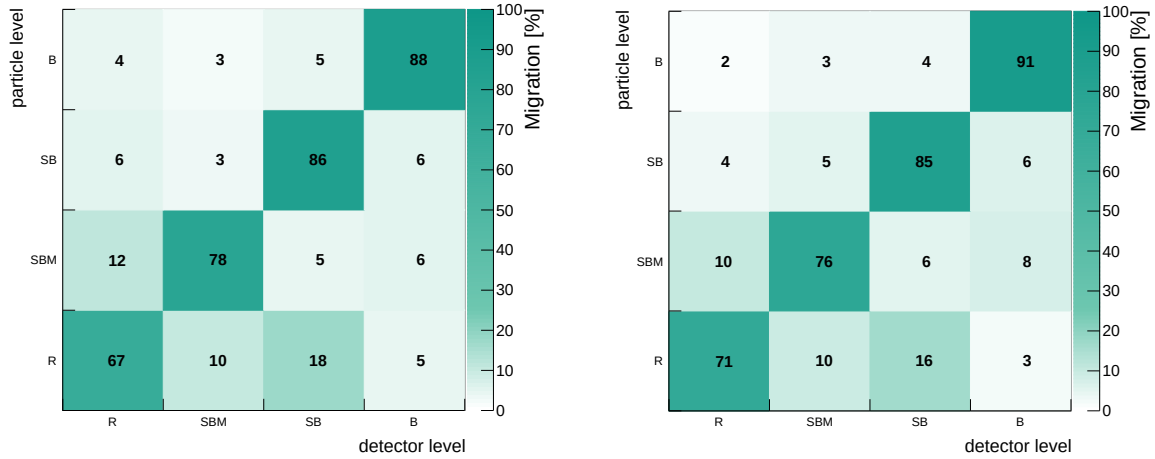

Figure 4: Migration of reconstructed events between reconstructed levels and topologies for samples with $M_{Z'} = 700$ GeV (left) and $M_{y_0} = 700$ (right).

Topology Event Fractions and Resolution

The reconstruction is performed independently at the detector and particle levels, thus it can lead to different reconstructed topology on each level. Migration of events between topologies and between the detector level (horizontal axis) and particle levels (vertical axis) is shown in Fig. 4 for the two main signal samples.

Contributions from particular topologies to the number of reconstructed events for different mass values of hypothetical particles in Fig. 5. The resolution for particular topologies can be extracted from widths of the mass spectra of the top anti-top quark pair and can be compared between topologies. The resolution of the spectra is wider at the detector level in general, which is expected due to the energy fluctuations of reconstructed jets in the simulated detector. However, the spectra are similar between the signal samples for both the particle and detector levels, although the peaks are wider for the sample with $My_0 = 700$ GeV.

The resolution for particular topologies can be extracted from widths of the mass spectra of the top anti-top quark pair and can be compared between topologies. The resolution of the spectra is wider at the detector level in general, which is expected due to the energy fluctuations of reconstructed jets in the simulated detector. However, the spectra are similar between the signal samples for both the particle and detector levels, although the peaks are wider for the sample with $My_0 = 700$ GeV.

The resolution was extracted as the width of the fitted of normal distribution, this information is shown in Fig. 6 in absolute values (a), b)) and relative values (c), d)) with respect to mass of hypothetical particle Z' (a), c)) and y_0 (b), d)). The Landau distribution was also tested for fitting, but the resulting error of fitting was larger than in case of fitting with normal distribution function. The resolution heavily depends on the combination of topology and mass of the studied hypothetical particle. For example the resolved topology has the best resolution for mass 500 GeV and then deteriorates with increasing mass. On the other hand, the boosted topology resolution performance has an opposite trend, where the samples with higher mass have better resolution for this topology, which corresponds to the increasing number of reconstructed events. In

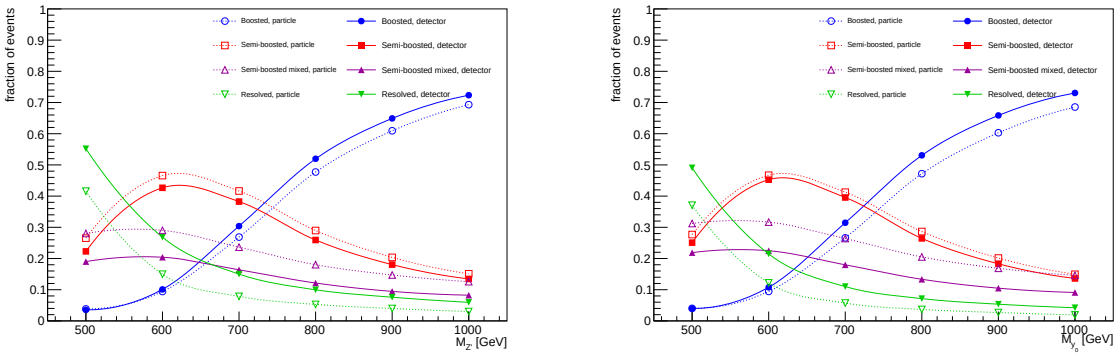

Figure 5: The fraction of events contributing to the $t\bar{t}$ reconstruction from each topology over samples with various masses of the hypothetical Z' (left) and y_0 (right) particle ($M_{Z'}$and M_{y_0}) at the detector (solid lines, full markers) and particle (dotted lines, open markers) levels.

general, the resolution is slightly better for the samples with Z' as probing particle.

The Unfolding Procedure and Signal Significance

The unfolding procedure and its performance on generated samples is presented in this section. The change in the strength of the hypothetical Z' or y_0 particle signal is studied before and after the unfolding procedure.

The first section describes the theory behind the unfolding procedure, followed by definition of the significance of the signal. Results of closure tests and the check of the unfolding procedure performance are presented before the results with chosen variables and samples are shown. Final results of the unfolding procedure are performed on an admixture of the signal Z' or y_0 sample, the $t\bar{t}$ sample and two background samples. Finally the comparison of significances between different topologies is described in the last section.

Unfolding Procedure

Spectra measured in every detector suffer in precision by the influences of the detector, in our case the simulation of the ATLAS detector. The unfolding procedure corrects for these influences, for example resolution of the detector and granularity of the separate subdetectors. There are several unfolding methods, which could possibly yield different results. The Fully Bayesian Unfolding (FBU) is chosen to mediate the unfolding procedure and was performed by the PyMC3 package [16, 17]. The FBU method estimates the probability density functions (posteriors) from the detector level spectrum values in each bin (priors) under conditions given by correction factors and the migration matrix. The most probable value in each bin can be taken as the unfolded value of the spectra of interest in the bin coresponding to the particle level spectrum. Among the main advantages of this method are that the migration matrix is not modified as in the singular value decomposition [18], absence of iterations in calculation in comparison with iterative unfolding [19], which also uses the Bayesian theorem, and the control over the result as all extremes of the probability density function are revealed

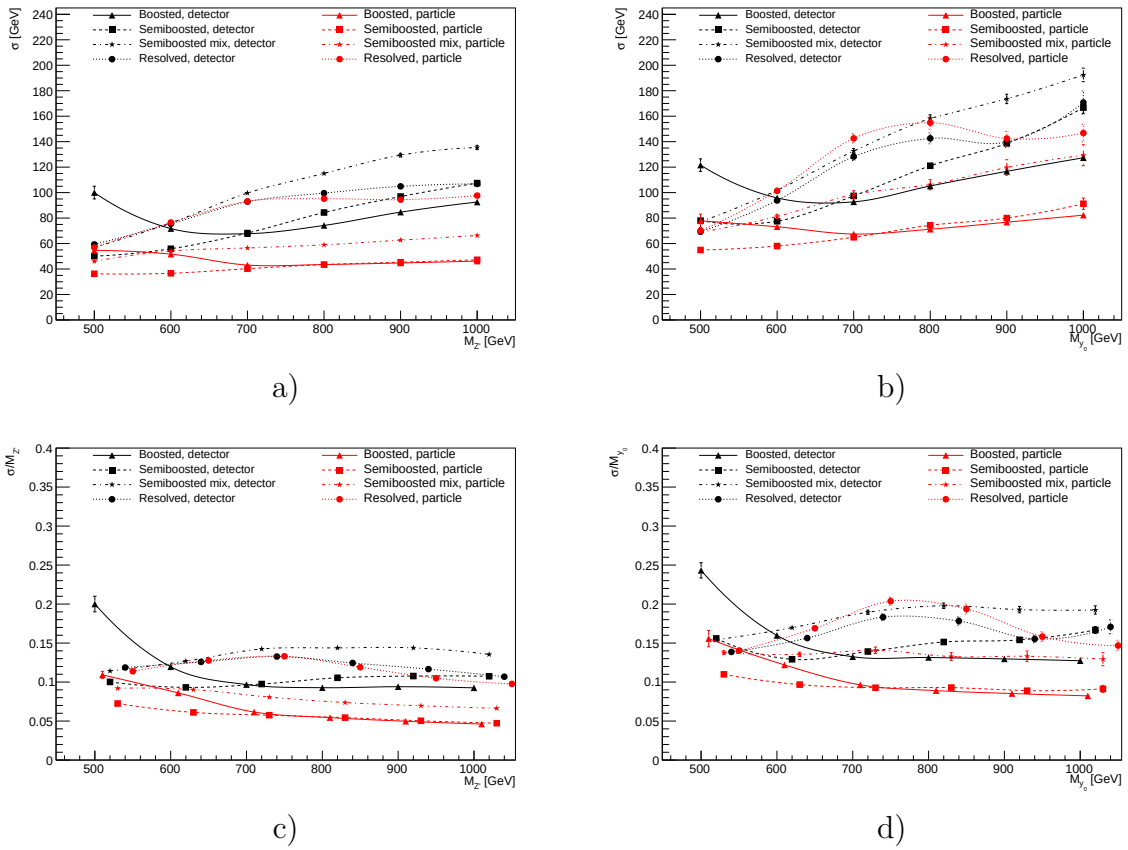

Figure 6: Comparison of the $t\bar{t}$ resolution for samples with different mass of hypothetical particle Z' (a),c)) and y_0 (b),d)) in particular topologies in absolute values (a), b)) and relative values (c),d).

and not only the one to which the procedure converges as in the iterative Bayesian unfolding. A general unfolding process is described by the following formula

$$\hat{T_{\mathrm{i}}} = \frac{1}{f_{\mathrm{i,eff}}} M^{-1}_{\mathrm{ij}} f_{\mathrm{j,acc}} (D_{\mathrm{j}} - B_{\mathrm{j}}), \tag{6}$$

where $\hat{T_{\mathrm{i}}}$ is the estimated value in the bin i of the particle level spectrum, $f_{\mathrm{i,eff}}$ and $f_{\mathrm{j,acc}}$ are efficiency and acceptance correction factors, defined in the next formula, M^{-1}_{ij} is embodiment of the unfolding procedure [3], D_{j} is the measured detector level spectra in bin j and finally B_{j} is the subtracted background contribution to the measured detector level spectrum. The efficiency and acceptance correction factors are defined as follows

$$f_{\mathrm{i,eff}} = \frac{P^{\mathrm{match}}_{\mathrm{t\bar{t},i}}}{P_{\mathrm{t\bar{t},i}}} \quad \text{and} \quad f_{\mathrm{j,acc}} = \frac{D^{\mathrm{match}}_{\mathrm{t\bar{t},j}}}{D_{\mathrm{t\bar{t},j}}}, \tag{7}$$

where $P^{\mathrm{match}}_{\mathrm{t\bar{t},i}}$ is the particle level spectrum value in bin i, which fulfills the particle level selection criteria and its detector level matched counterpart fulfills the detector level selection criteria; $P_{\mathrm{t\bar{t},i}}$ is the particle level spectrum value in bin i, which fulfill the particle level selection criteria regardless on its detector level counterpart, both evaluated on the $t\bar{t}$ sample. Similarly, $D^{\mathrm{match}}_{\mathrm{t\bar{t},j}}$ is the detector level spectrum value in bin j fulfilling particle level selection criteria and is matched to the detector level counterpart and $D_{\mathrm{t\bar{t},j}}$ is reconstructed detector level spectrum value in bin j without any matching to the particle level counterpart, both evaluated on the $t\bar{t}$ sample. The events contributing to the matched spectra are fulfilling the corresponding selection criteria and are reconstructed at both detector and particle levels in the same topology, thus the matching descriptor.

Significance of the Signal before and after the Unfolding

The spectra entering the unfolding procedure have the addition of the Z' or y_0 signal sample with an amplified cross section by an ad hoc number ($5 * 10^5$ and 300 respectively) to study the impact of the unfolding on the strength of the signal. The strength of the signal is quantified by a significance, which considers statistical errors of used samples in the given bin. The signal significance S in the given bin i before unfolding is defined for the hypothetical particle Z' as

$$S_{i,\mathrm{det}} = (P^{t\bar{t}+Z'+Bg}_{\mathrm{i}} - T^{t\bar{t}}_{\mathrm{i}} - Bg_{\mathrm{i},1} - ... - Bg_{\mathrm{i},n})/(\sqrt{\sigma^2_{P_{\mathrm{i}}} + \sigma^2_{T_{\mathrm{i}}}}), \tag{8}$$

where P_{i} are the pseudo data consisting from the signal and the background added to the expected $t\bar{t}$ sample in the given bin, T_{i} is the detector level spectrum from the statistically independent $t\bar{t}$ sample and $Bg_{\mathrm{i},n}$ is the background contribution to the studied spectra from the n-th background sample, $\sigma_{P_{\mathrm{i}}}$ is the statistical error of the pseudo data sample in the given bin and $\sigma_{T_{\mathrm{i}}}$ is the statistical error of the bin value of the statistically independent $t\bar{t}$ sample.

A similar significance is defined after the unfolding procedure

$$S_{i,\mathrm{unf}} = (U^{t\bar{t}+Z'}_{\mathrm{i}} - T^{t\bar{t}}_{\mathrm{i}})/(\sqrt{\sigma_{U^2_{\mathrm{i}}} + \sigma^2_{T_{\mathrm{i}}}}), \tag{9}$$

[3] The FBU unfolding does not use inverted migration matrix. The notation is traditional way to incorporated the unfolding procedure in the formula.

where U_{i} are the unfolded data in the given bin, T_{i} is the particle level spectrum from the statistically independent $t\bar{t}$ sample, $\sigma_{U_{\mathrm{i}}}$ is the statistical error of the unfolded spectra in the given bin and $\sigma_{T_{\mathrm{i}}}$ is the statistical error of bin value of the statistically independent $t\bar{t}$ sample.

The detector and the unfolded significance plots are shown under the ratio plots in the unfolded spectra.

The integral significance, strength of the signal over the whole spectrum, is defined similarly for both the detector and the unfolded level. The detector integral significance is defined as

$$S_{\mathrm{I,det}} = \sum_{i=0}^{m} (P_{\mathrm{i}}^{t\bar{t}+Z'+Bg} - T_{\mathrm{i}}^{t\bar{t}} - Bg_{\mathrm{i},1} - ... - Bg_{\mathrm{i},n}) / \sqrt{\sum_{i=0}^{m} (\sigma_{P_{\mathrm{i}}}^2 + \sigma_{T_{\mathrm{i}}}^2)}, \tag{10}$$

where m is the number of bins in the given spectrum, P_{i} are the pseudo data consisting from the signal and the background added to the expected $t\bar{t}$ sample in the given bin, T_{i} is the detector level spectrum from the statistically independent $t\bar{t}$ sample and $Bg_{\mathrm{i},n}$ is the background contribution to the studied spectra from the n-th background sample, $\sigma_{P_{\mathrm{i}}}$ is the statistical error of the pseudo data sample in the given bin and $\sigma_{T_{\mathrm{i}}}$ is the statistical error of bin value of the statistically independent $t\bar{t}$ sample.

The detector integral significance is the same for all variables for given particle, *i.e.* the $M^{\mathrm{t\bar{t}}}$ spectrum and $p_{\mathrm{T}}^{\mathrm{t\bar{t}}}$ spectrum have the same value of the detector integral significance.

The integral significance for unfolded level or unfolded integral significance is defined similarly as

$$S_{\mathrm{I,unf}} = \sum_{i=0}^{m} (U_{\mathrm{i}}^{t\bar{t}+Z'} - T_{\mathrm{i}}^{t\bar{t}}) / \sqrt{\sum_{i=0}^{m} (\sigma_{U_{\mathrm{i}}^2} + \sigma_{T_{\mathrm{i}}}^2)}, \tag{11}$$

where m is number of bins in the given spectrum, U_{i} are the unfolded data in the given bin, T_{i} is the particle level spectrum from the statistically independent $t\bar{t}$ sample, $\sigma_{U_{\mathrm{i}}}$ is the statistical uncertainty of the unfolded spectra in the given bin and $\sigma_{T_{\mathrm{i}}}$ is the statistical error of bin value of the statistically independent $t\bar{t}$ sample.

The unfolded integral significance is varying slightly as the unfolding procedure is not able to reproduce exactly the same results but the resulting quantities are slightly shifting in the range of statistical error. Significances for the hypothetical particle y_0 are defined in the same manner as for the Z' particle.

The uncertainty of the detector level significance is estimated from 100 pseudoexperiments, where the detector level spectrum is smeared in each bin with the random number taken from a gaussian curve with the σ parameter set to the statistical uncertainty of the studied bin and mean parameter set to zero value. Pseudoexperiment values are then studied in each bin fitted by a gaussian curve and its σ parameter is the detector level significance uncertainty for the given bin. The unfolded significance uncertainty estimation is performed in a similar way, the spectrum is first smeared at the detector level and then unfolded and each bin is studied as in the detector level significance uncertainty estimation case.

Unfolding with Background

The results for the unfolding of the signal samples with hypothetical particles Z' and y_0 are presented in this section for chosen variables. The focus is set to the samples with $M_{Z'} = 700$ and $M_{y_0} = 700$ where the studied semi-boosted topologies fraction of events is high. The transverse momentum and cosine of the production angle of the hadronically decaying top quark ($p_T^{t,had}$ and $\cos\theta^*_{t,had}$) are chosen for examples of the unfolding procedure in the semi-boosted topology. The first step in the unfolding process is to mix spectra with background and $t\bar{t}$ sample and weight them to same luminosity, the luminosity of the $t\bar{t}$ sample was used in our case. The resulting mixed spectra entering the unfolding are shown in Fig. 7 for the aforementioned variables. The black dotted spectrum corresponds to the same mixed spectra from the statistically independent sample part for verification of the mixed spectrum.

The ad hoc weighting parameter of signal samples was introduced to scale up the normalization of the sinal. Signal samples would have small fraction of events due to their small cross section. An add hoc scaling parameter is set to 300 for the samples with hypothetical particle y_0 and further by five for the resolved topology for the sample with $M_{y_0} = 700$ GeV. The value of this parameter for the sample with $M_{Z'} = 700$ GeV is set to 10 000 for all topologies.

Bin-by-bin corrections, also known as acceptance and efficiency corrections, are essential for unfolding as they correct for two phenomena. First, at the the detector level by removing non-signal events and at the particle level for undetected events. Those corrections are evaluated on the $t\bar{t}$ sample based on the equations shown in section. The $t\bar{t}$ sample was used for the determination of the corrections to increase correspondence to the real measurements for searches of unknown particles in the top quark spectra. Bin-by-bin migration of events between the detector and the particle levels is described by the migration matrix separately for each topology. Migration matrices are evaluated on the $t\bar{t}$ sample to achieve consistency with acceptance and efficiency corrections.

The results from the unfolding procedure for the chosen variables, namely the transverse momentum ($p_T^{t,had}$) and cosine of the production angle of hadronically decaying top quark ($\cos\theta^*_{t,had}$) are shown in Fig. 8. The unfolding results are compared with detector level spectra corrected for the acceptance and efficiency to show the influence of the unfolding in the spectra in the top pad. The ratio between the unfolded and particle level spectra from the statistically independent sample is shown in middle tab. The bottom part of each plot shows the detector and unfolded significances, in general, the signal is stronger in the spectrum before unfolding than in the unfolded spectrum. This phenomenon manifests over all samples, topologies and variables, with exception for the cosine of the production angle of hadronically decaying top quark spectrum in the boosted topology.

The unfolding results show good agreement in the "closure" chi-squared test ($\chi^2_{t\bar{t}+Z'}$ and $\chi^2_{t\bar{t}+y_0}$), while the chi-squared test between unfolded and $t\bar{t}$ shows non-negligible influence of the signal. In general, the detector significance is higher in all studied spectra of all variables in all samples and topologies. This is manly caused by the difference between detector level spectra statistical uncertainty and width of the posteriors in the unfolding procedure, which is larger roughly by factor of two and is discussed in the next section.

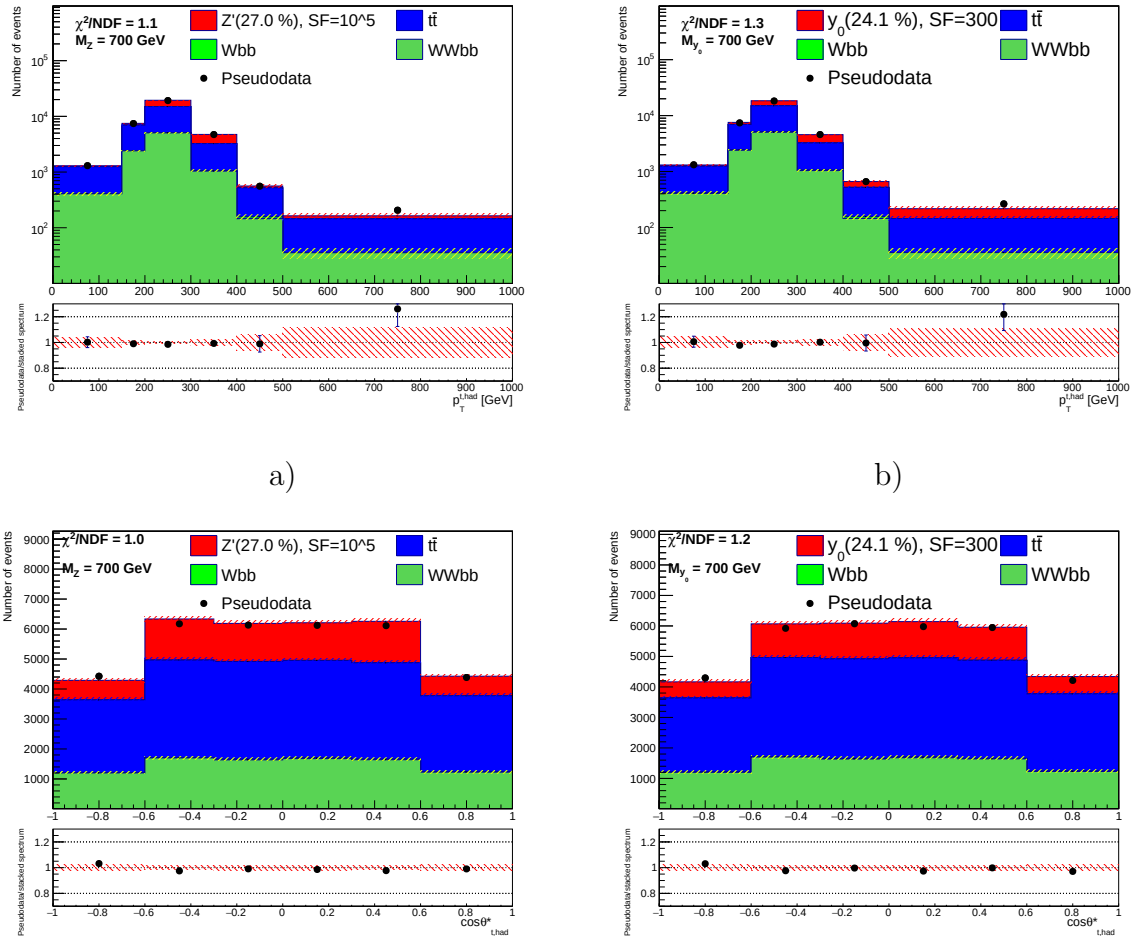

Figure 7: Comparison of the detector level spectra from two statistically independent parts (full markers and filled stack) for the $t\bar{t}$ sample with the addition of Wbb and $WWbb$ backgrounds and an admixture of events from the sample with $M_{\mathrm{y_0}} = 700$ GeV (a), c)) and the sample with $M_{\mathrm{Z'}} = 700$ GeV (b), d)) for the transverse momentum of the hadronically decaying top quark ($p_{\mathrm{T}}^{\mathrm{t,had}}$, a), b)) and for the cosine of the production angle of the hadronically decaying top quark ($\cos\theta^*_{\mathrm{t,had}}$, c), d)), all spectra are reconstructed in the semi-boosted topology. The hatched bands in the top panel represent the statistical uncertainty in each sample.

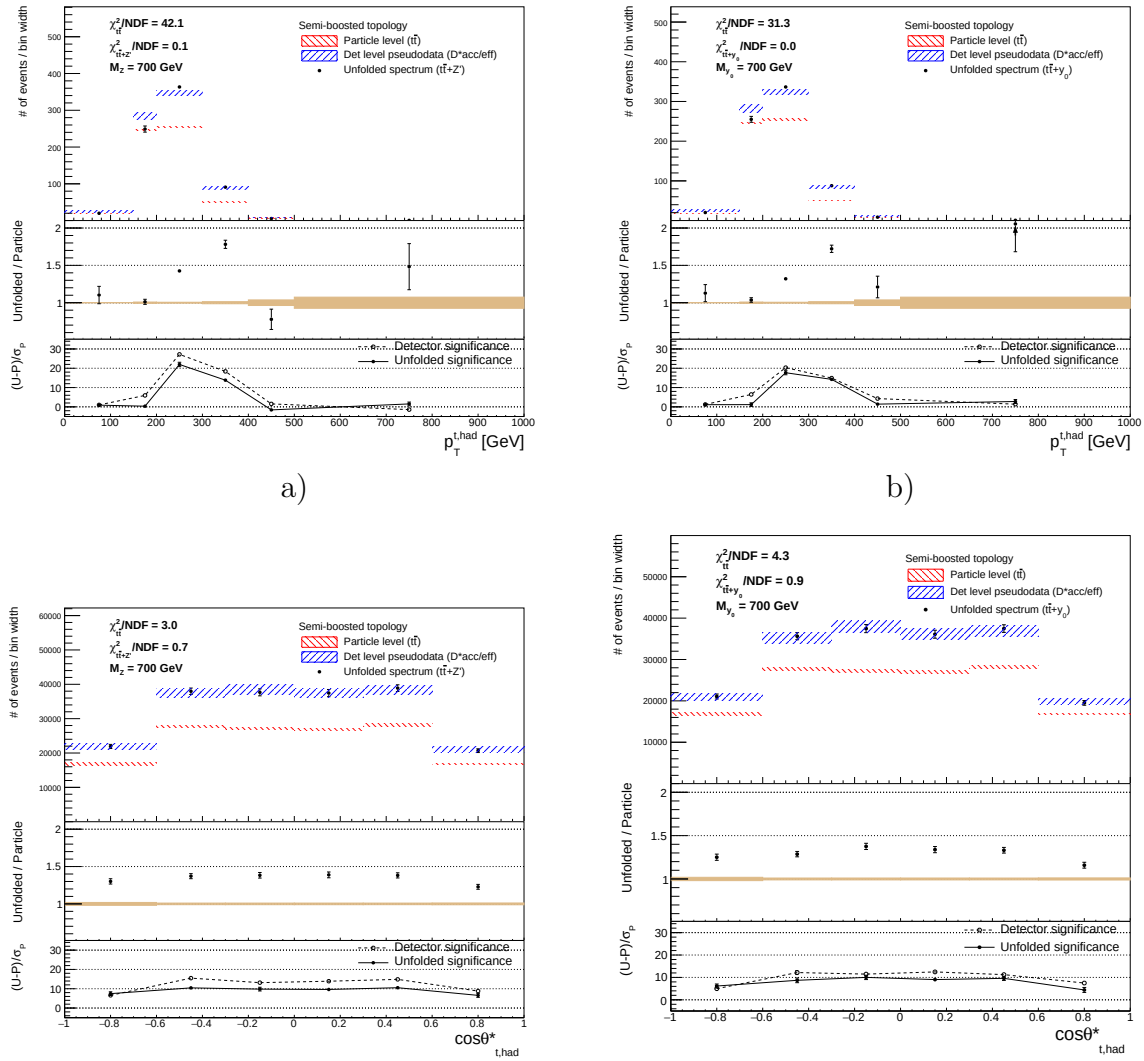

Figure 8: Unfolding results for the rapidity of the hadronically decaying top quark $p_{\mathrm{T}}^{\mathrm{t,had}}$ (a), b)) and for the cosine of the production angle of the hadronically decaying top quark $\cos\theta^{*}_{\mathrm{t,had}}$ (c), d)) for samples with mass of the hypothetical particle $M_{\mathrm{Z'}} = 700$ GeV (a), c)) and $M_{\mathrm{y_0}} = 700$ GeV (b), d)) all in the semi-boosted topology. The top part of each plot shows unfolding results on the admixture of spectra (black full markers) compared with the particle level spectrum from statistically independent sample (red) and with detector level spectrum from $t\bar{t}$ sample (blue) corrected by the acceptance and efficiency factors to achieve similar phase space. The hatched area corresponds to the statistical uncertainty of the spectrum. The $\chi^2_{\mathrm{t\bar{t}}}$ test is performed between $t\bar{t}$ particle level spectrum and unfolded spectrum while $\chi^2_{\mathrm{t\bar{t}+Z'}}$ and $\chi^2_{\mathrm{t\bar{t}+y_0}}$ are performed between unfolded and $t\bar{t}$ particle level spectrum with respective signal particle level addition (closure test). The middle part of each plot shows the ratio between the unfolded spectrum and the particle level spectrum one from the statistically independent $t\bar{t}$ sample only. The yellow bar area shows the statistical uncertainty of the particle level spectra of the $t\bar{t}$ sample. The bottom part of the plot shows comparison between the unfolded (full markers, solid line) and the detector level (open markers, dashed line) significances.

Significance of the Signal and Influence of Unfolding Procedure

The significance of the signal with respect to the $t\bar{t}$ sample is evaluated on the detector and unfolded levels by using formula from previous section. The uncertainty of the significance is evaluated using 100 pseudoexperiments, which are unfolded afterwards. Each pseudoexperiment spectrum is prepared from the admixture of spectra entering the unfolding by smearing content in each bin by amount randomly picked from the statistical uncertainty interval. The gaussian distribution function is used for the random selection of the smearing value from the aforementioned interval.

Each pseudoexperiment results in a slightly different significance due to the smearing of the spectrum, thus, calculated significances for each pseudoexperiment differ. The distribution of significances in each bin is then fitted by a gaussian function and width of this fit is considered as statistical uncertainty of the significance in each bin. Distribution of the significances extracted from unfolded pseudoexperiments is shown in Fig. 9 for the transverse momentum of the hadronically decaying top quark $p_{\mathrm{T}}^{\mathrm{t,had}}$ and for the cosine of the production angle of the hadronically decaying top quark $\cos\theta^{*}_{\mathrm{t,had}}$, both in the semi-boosted topology.

Results on Significance

The signal significances in the $p_{\mathrm{T}}^{\mathrm{t,had}}$ spectrum peaks at different values of $p_{\mathrm{T}}^{\mathrm{t,had}}$ depending on the topology as the event selection in each topology biases the spectrum and effectively selects different ranges in $M_{\mathrm{t\bar{t}}}$, too. On the other hand, significance in the $M_{\mathrm{t\bar{t}}}$ spectrum peaks around the value of the generated y_0 mass or Z' mass of 700 GeV as expected, with a slight tail to lower values in the resolved topology which is the least suitable one to reconstruct a resonance of such a large mass. In contrast, the $y_{\mathrm{t,had}}$ and the $\cos\theta^{*}_{\mathrm{t,had}}$ signal significance is very flat also for the signal sample and there is no clear isolated excess of signal events in this spectrum, with the exception of the boosted topology which selects, by construction, high-p_{T} large jets and thus also top quarks, consequently more localized in the central rapidity region, producing a peak around zero, shown in Fig 9.

The four selected spectra are thus good candidate observables to illustrate different behavior and spread of significances over bins, also presenting a selection of observables of a dimension of energy as well as dimensionless (angular). The binned significances are in general lower after the unfolding, for which an explicit proof is delivered by this study. The cause of this is as follows.

While a sharper spectrum may be recovered by unfolding, the procedure in general correlates information among bins by maximizing a likelihood function in case of FBU, or minimizing (possibly modified and regularized) χ^2 or iterating and sequentially improving the result for the case of other methods. An increase in the correlation across bins of the unfolded spectrum is a known and important fact and a correlation matrix should preferably be published along with unfolded spectra from real experiments, as done *e.g.* in [20, 21] where a correlation matrix between the observables was also evaluated. We observe that in case of the FBU method the posteriors variance usually increases, leading to larger absolute as well as relative uncertainties of the unfolded spectrum w.r.t. the particle level one. This effectively decreases the significance of the observed signal excess. An increase of the statistical uncertainties with the number of iterations in case of the Iterative Bayesian Unfolding [19] was also reported by other

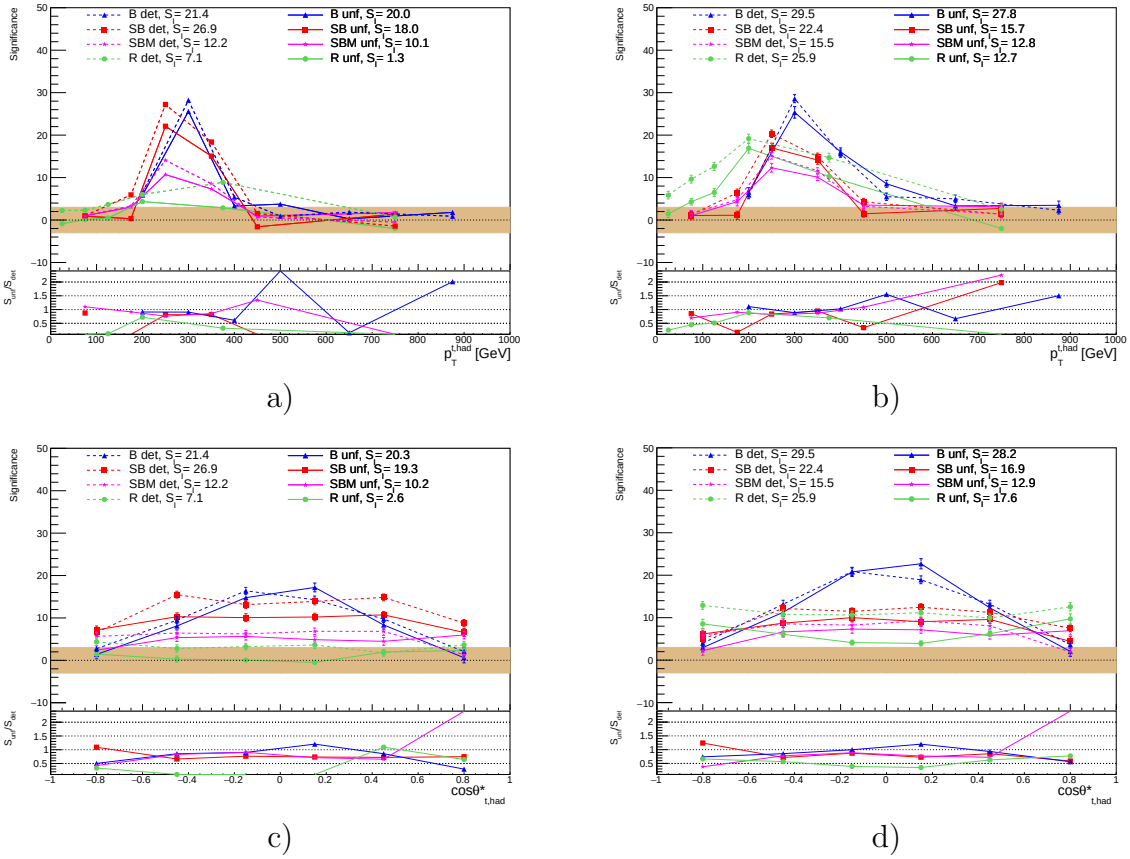

Figure 9: The detector (open markers, dashed line) and unfolded (full markers, solid line) significances for the rapidity of the hadronically decaying top quark ($y_{\mathrm{t,had}}$, a), b)) and the cosine of the production angle of the hadronically decaying top quark ($\cos\theta^*_{\mathrm{t,had}}$, c), d)) plotted for all the topologies in each bin for samples with mass of the hypothetical particle $M_{\mathrm{Z'}} = 700$ GeV (a), c)) and $M_{\mathrm{y_0}} = 700$ GeV (b), d)). The band defines the area where the absolute value of the significance is below three, corresponding to the 3-σ interval. The lower pads present the ratios of the unfolded over the detector level significances, without uncertainties which are highly correlated.

analyses [22]. We note that in our case the BSM signal significances decrease by 20–40%.

Conclusions

The results of the $t\bar{t}$ spectra shapes, their resolution and hypothetical BSM signal significance studies in the ℓ + jets channel on simulated signal and background samples were presented in this work. The selection criteria are chosen as close to the real analyses as possible corresponding to the ATLAS top working group analysis, thus, the mutual comparison is possible. The addition of the semi-boosted and semi-boosted mixed topology enhances yields between 20% and 50% in the $t\bar{t}$ mass range from 500 GeV to 1000 GeV. The resolution of the reconstructed $t\bar{t}$ mass peak at the detector level in the semi-boosted topology is comparable with the resolution for boosted and resolved topology. The semi-boosted mixed topology has slightly worse resolution, roughly by 50%. The results of the unfolding procedure on the $t\bar{t}$ sample corresponds well to the simulated particle level in closure tests as well as with the addition of the weighted background samples and hypothetical Z' and y_0 particles signal samples. The strength of the signal quantified by the significance is well visible after the unfolding in the admixture of the $t\bar{t}$, background and the hypothetical particle sample. However, the significance is diminished by the unfolding procedure for spectra of transverse momentum of hadronically decaying top quark, reconstructed top anti-top quark mass and production angle with the exception for angular variables in the boosted topology. Namely, the cosine of the production angle and the rapidity show only a small gap between the detector and unfolded significances for both hypothetical particles. This phenomenon is not visible for other topologies in samples, where these topologies have dominant fraction of events, for example in the sample with $m_{Z'} = 700$ GeV for the semi-boosted topology. The explanation lies in the ingredients of the unfolding procedure, where the migration matrix of the angular variables is diagonal and the events does not migrate in large numbers between the bins. The width of the posterior in unfolding in the studied bin is then smaller, which leads to the lesser diminishing of the signal. Unfolding procedure also strengthens the peak in spectra and combination of those two factors may lead to the higher significance at the unfolded level for the cosine of the production angle. This quantification of the significance of the signal before and after unfolding is, to our knowledge, fully demonstrated for the first time in this study. The unfolded spectra results still show sensitivity to the presence of the possible BSM signal is the $t\bar{t}$ spectrum.

Acknowledgments

The author gratefully acknowledges the support from following projects: Research Infrastructure for experiments at CERN, LM2018104, Getting new knowledge of the microworld using the CERN infrastructure, MSMT CERN TRANSFER_UP LTT17018, Czech Science Foundation project GAČR 19-21484S and Palacky University scholarship program Student Mobility - Traineeship.

Bibliography

[1] Gregorio Bernardi, T. R. Junk, and M. Carena. Higgs bosons, theory and searches. 2008.

[2] Georges Aad et al. Measurements of the Higgs boson production and decay rates and constraints on its couplings from a combined ATLAS and CMS analysis of the LHC pp collision data at $\sqrt{s} = 7$ and 8 TeV. *JHEP*, 08:045, 2016.

[3] A detailed map of Higgs boson interactions by the ATLAS experiment ten years after the discovery. *Nature*, 607(7917):52–59, 2022.

[4] Wikimedia Commons. File:standard model of elementary particles.svg — wikimedia commons, the free media repository, 2022. [Online; accessed 18-December-2022].

[5] CDF experiment collaboration. Observation of top quark production in $\bar{\text{p}}$p collisions with the collider detector at fermilab. *Phys. Rev. Lett.*, 74:2626–2631, Apr 1995.

[6] D0 Experment Collaboration. Observation of the top quark. *Phys. Rev. Lett.*, 74:2632–2637, Apr 1995.

[7] Combination of ATLAS and CMS results on the mass of the top quark using up to 4.9 inverse femtobarns of data. 2013.

[8] R. L. Workman and Others. Review of Particle Physics. *PTEP*, 2022:083C01, 2022.

[9] Giuseppe Degrassi, Stefano Di Vita, Joan Elias-Miró, José R. Espinosa, Gian F. Giudice, Gino Isidori, and Alessandro Strumia. Higgs mass and vacuum stability in the standard model at nnlo. *Journal of High Energy Physics*, 2012(8), 2012.

[10] Georges Aad et al. Topological cell clustering in the ATLAS calorimeters and its performance in LHC Run 1. *Eur. Phys. J. C*, 77:490, 2017.

[11] J. Alwall, R. Frederix, S. Frixione, V. Hirschi, F. Maltoni, O. Mattelaer, H. S. Shao, T. Stelzer, P. Torrielli, and M. Zaro. The automated computation of tree-level and next-to-leading order differential cross sections, and their matching to parton shower simulations. *JHEP*, 07:079, 2014.

[12] Duhr C. FeynRules Implementation of Abelian Higgs Model. 2011. `https://feynrules.irmp.ucl.ac.be/wiki/HiddenAbelianHiggsModel`.

[13] Neil D. Christensen and Claude Duhr. FeynRules - Feynman rules made easy. *Comput. Phys. Commun.*, 180:1614–1641, 2009.

[14] James D. Wells. How to Find a Hidden World at the Large Hadron Collider. 2008.

[15] Benjamin Nachman, Pascal Nef, Ariel Schwartzman, Maximilian Swiatlowski, and Chaowaroj Wanotayaroj. Jets from Jets: Re-clustering as a tool for large radius jet reconstruction and grooming at the LHC. *JHEP*, 02:075, 2015.

[16] John Salvatier, Thomas V Wiecki, and Christopher Fonnesbeck. Probabilistic programming in python using pymc3. *PeerJ Computer Science*, 2:e55, 2016.

[17] D. Gerbaudo. Implementation of the Fully Bayesian Unfolding. 2019. `https://github.com/gerbaudo/fbu`.

[18] Andreas Höcker and Vakhtang Kartvelishvili. Svd approach to data unfolding. *Nuclear Instruments and Methods in Physics Research Section A: Accelerators, Spectrometers, Detectors and Associated Equipment*, 372(3):469–481, Apr 1996.

[19] G. D'Agostini. Improved iterative bayesian unfolding. `https://arxiv.org/abs/1010.0632`, 2010.

[20] Georges Aad et al. Measurements of normalized differential cross sections for $t\bar{t}$ production in pp collisions at $\sqrt{s} = 7$ TeV using the ATLAS detector. *Phys. Rev. D*, 90(7):072004, 2014.

[21] M. Aaboud, G. Aad, B. Abbott, J. Abdallah, O. Abdinov, Baptiste Abeloos, S. Abidi, O. AbouZeid, Nicola Abraham, H. Abramowicz, Heather Abreu, Ricardo Abreu, Y. Abulaiti, Basanta Acharya, S. Adachi, L. Adamczyk, J. Adelman, Michael Adersberger, T. Adye, and L. Zwalinski. Measurements of top-quark pair differential cross-sections in the lepton+jets channel in *pp* collisions at $\sqrt{s} = 13$ tev using the atlas detector. *Journal of High Energy Physics*, 2017, 11 2017.

[22] Georges Aad et al. Differential top-antitop cross-section measurements as a function of observables constructed from final-state particles using pp collisions at $\sqrt{s} = 7$ TeV in the ATLAS detector. *JHEP*, 06:100, 2015.